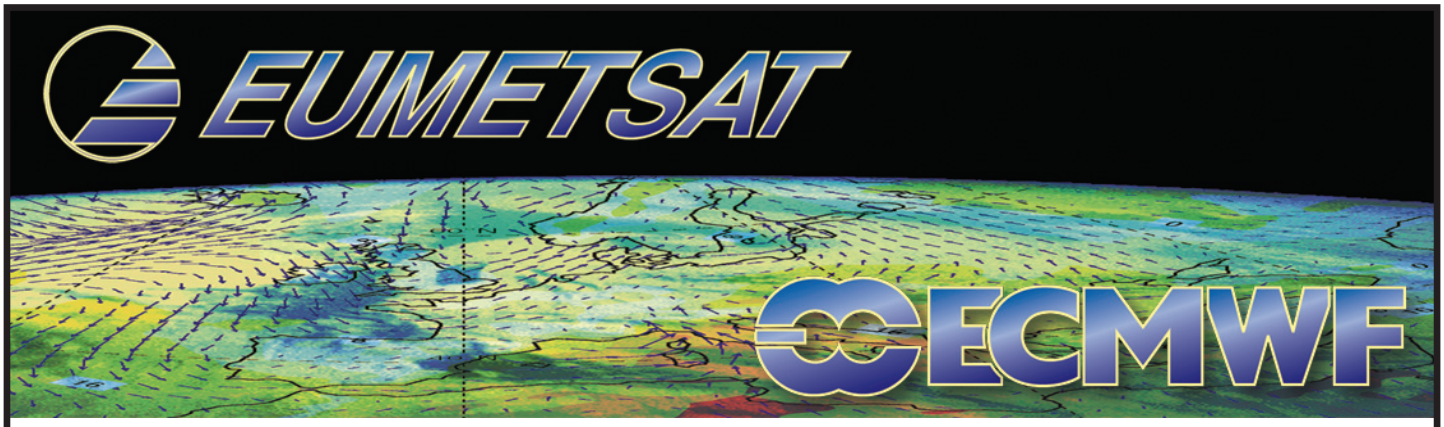

EUMETSAT/ECMWF Fellowship Programme
Research Report No. 44

Effect of assimilating microwave imager observations in the presence of a model bias in marine stratocumulus

Katrin Lonitz and Alan Geer

March 2017

Series: EUMETSAT/ECMWF Fellowship Programme Research Reports

A full list of ECMWF Publications can be found on our web site under:
http://www.ecmwf.int/publications/

Contact: library@ecmwf.int

European Centre for Medium Range Weather Forecasts
Shinfield Park, Reading, RG2 9AX, England

Abstract

Decks of stratocumulus clouds over the easternmost parts of the maritime continent show a positive bias in the microwave brightness temperatures in the order of a Kelvin. We think the cause of this bias is an insufficient representation of drizzle and cloud liquid water path in the forecast model under stable conditions and an insufficient amplitude of cloud or drizzle diurnal variation in stratocumulus areas. This bias is not easy to correct with variational bias correction so biases in stratocumulus regions remain and are being assimilated, which led to concerns that these could have potentially affected the quality of the forecast. The most recent model cycle 43R1 of the Integrated Forecast System generates more stratocumulus clouds through a change in the entrainment in the shallow convection scheme, which corrects part of the bias. In this study, the estimated inversion strength is shown to be a good measure to identify and screen stratocumulus clouds before being assimilated. With such a screening the root-mean-square errors in relative humidity and temperature are reduced, which is caused by a change in the analysis and in the short-range forecast in very localised stratocumulus areas. Medium-range forecast scores are unaffected. Furthermore, fits to other humidity sensitive observations are slightly degraded by the screening. Hence, microwave observations in stratocumulus areas are probably useful for the assimilation system and should not be screened, despite the presence of biases.

1 Motivation

Maritime stratocumulus clouds are most prominent in the easternmost parts of the Atlantic and Pacific, close to the coasts of North and South America and Africa. On average, there are positive normalised First Guess (FG) departures as shown as red coloured areas in Fig. 1a in 37 GHz, v-polarised (37v) radiances from Special Sensor Microwave Imager/Sounder F-17 (SSMIS F-17), which is very sensitive to cloud water, drizzle, rain, humidity and the sea surface. Areas with high values in normalised FG departure correspond to areas where the biases (observation - FG) are large relative to their observation error. That means, positive biases in these areas can really have an effect on the analysis (and forecast). This positive bias is also clearly seen in the 89v channel, which is even more sensitive to liquid water (cloud and drizzle). For 19 GHz, which is sensitive to larger droplets and rain, the bias is not present (not shown). As illustrated in Fig. 1b, the low-peaking (around 5 km height) water vapour sounding channel 183$\pm$6.6 GHz shows a slightly negative bias in those areas (which is consistent with the positive bias in the imager channels) suggesting the model has slightly lower water vapour content or less cloud than observations.

Kazumori et al. (2016) investigated the behaviour of biases in stratocumulus in more detail using various microwave imagers (AMSR2, SSMIS F-16, F-17 and F-18, Windsat and TMI), which observe these regions at different local times. They found that the biases of FG departure show a dependence on local time in areas of stratocumulus, especially during summer. Here, the positive bias has its peak during night-time (see their Fig. 15). Kazumori et al. (2016) believe that both the liquid water diurnal variation and the liquid water amount were underestimated by the model in these cases. However, there is also the chance that the treatment or amount of drizzle in the model and observation operator is not optimal.

Fig. 2 illustrates how the bias in stratocumulus has changed with the newest operational model cycle 43R1 (Fig. 2b) which generates more stratocumulus clouds through a change in the entrainment in the shallow convection scheme (personal communication with Peter Bechtold, see also Buizza et al., 2017) and corrects part of the bias in stratocumulus compared to a previous IFS cycle 41R2 (Fig. 2a). However, in areas of stratocumulus clouds the IFS model seems still not to have enough drizzle or cloud liquid water compared to observations (especially seen at the West coast of Africa in Fig. 2).

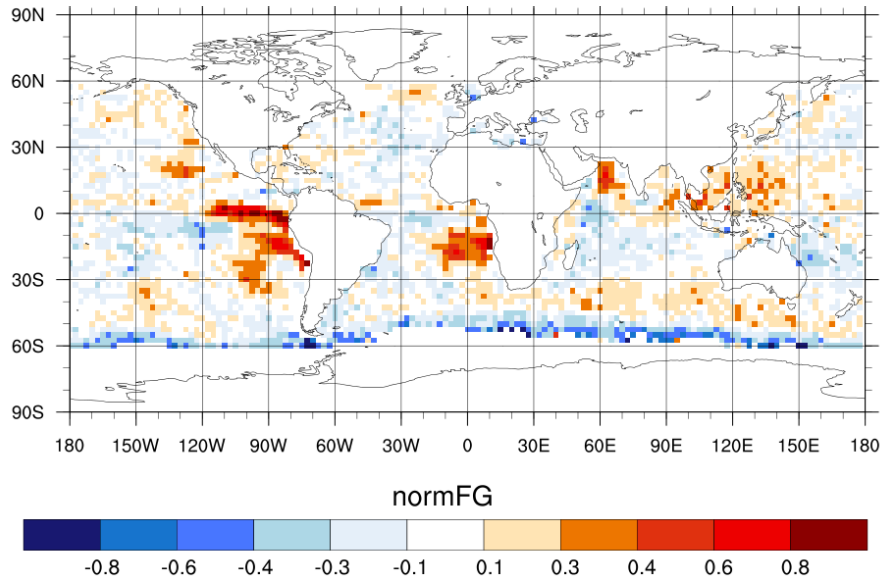

(a) 37 GHz, v-polarised

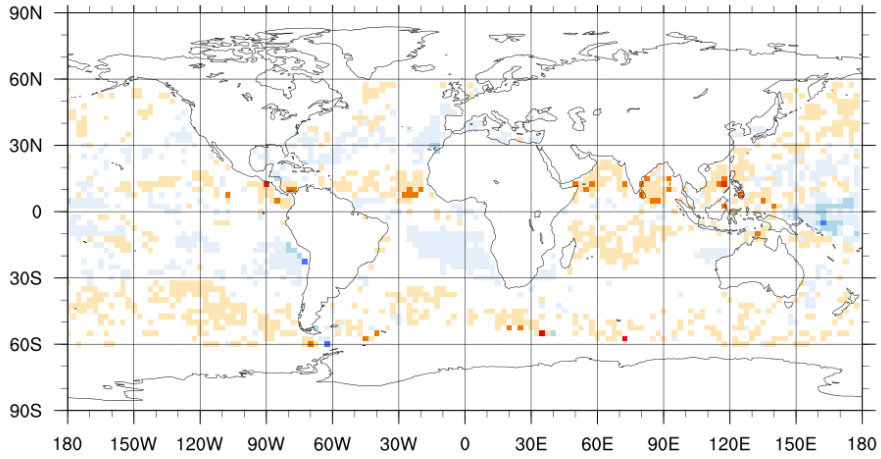

(b) 183±6.6 GHz

Figure 1: Map of monthly mean gridded (2.5°lat x 2.5°lon) normalised FG departures (FG departures divided by observation error) for SSMIS F-17 at a) 37 GHz, v-polarised and b) 183±6.6 GHz for August 2013 using IFS cycle 40R2.

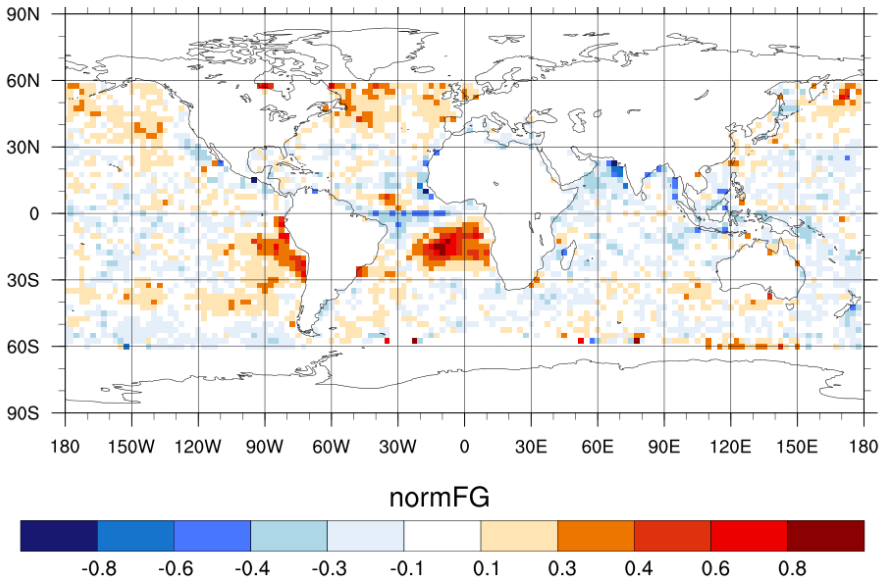

(a) IFS cycle 41R2

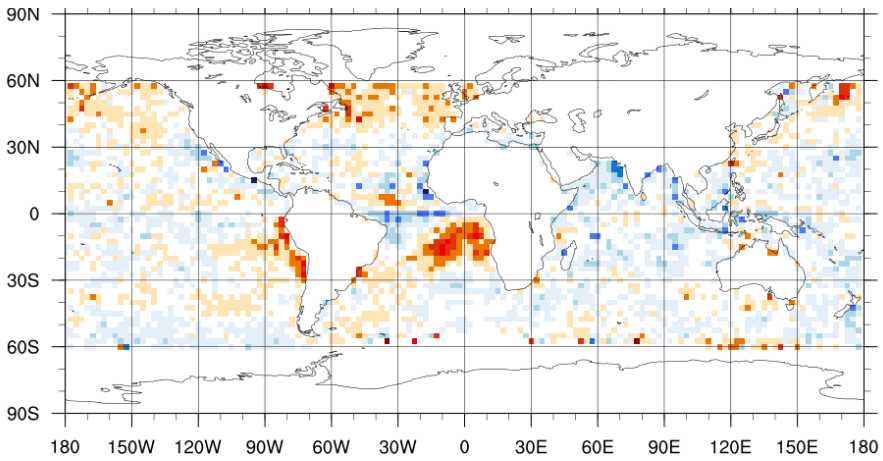

(b) IFS cycle 43R1

Figure 2: Map of monthly mean gridded (2.5°lat x 2.5°lon) normalised FG departures (FG departures divided by observation error) for SSMIS F-17 at 37 GHz, v-polarised for November 2015 based on experiments in TCo399 using IFS cycle a) 41R2 and b) 43R1.

Usually, systematic biases are treated by the variational bias correction (VarBC), however, in stratocumulus regions VarBC does not remove this bias sufficiently. This is because no predictors inside VarBC exist which target the bias in stratocumulus areas. If no such predictor is available, the observational data would usually be screened out before being assimilated. This is done e.g. for cold-air outbreak regions in the southern hemisphere, where the model generates too much ice instead of liquid water (Lonitz and Geer, 2015). However, no screening of microwave imager (MWI) data in stratocumulus regions has been done until now. In this study, we explore if the estimated inversion strength (EIS) can be used as a VarBC predictor (section 2) and study the forecast impact of screening observations in stratocumulus areas (section 3).

2 Identification of stratocumulus regions

Stratocumulus clouds are located at the top of the planetary boundary layer, which is characterized by a strong inversion. Wood and Bretherton (2006) state that the estimated inversion strength (EIS) is a good estimate of the inversion strength of the planetary boundary layer and, therefore, can be used to identify stratocumulus regions in the model. The estimated inversion strength is defined as:

$$\mathrm{EIS} = \mathrm{LTS} - \Gamma_m^{850}(z_{700} - \mathrm{LCL}), \tag{1}$$

with the moist adiabatic potential temperature gradient at 850 hPa Γ_m^{850} [K m^{-1}], the height of the $p = 700\,hPa$ surface z_{700} [m], and the lifting condensation level LCL [m]. The LCL is the height at which an air-parcel is cooled by dry adiabatic lifting so its relative humidity reaches 100%. Furthermore, EIS depends on the lower-tropospheric stability (LTS) [K] (Slingo, 1987; Klein and Hartmann, 1993; Wood and Hartmann, 2006). LTS is the difference in potential temperature between the 700-hPa level and the surface, which is a good measure of the strength of the inversion that caps the planetary boundary layer [PBL] (Wood and Hartmann, 2006). The stronger the inversion the more effectively moisture can be trapped within the PBL allowing for a greater stratiform cloud cover. In other words, EIS [K] is a good measure for periods of moderate tropospheric subsidence, which is related to the formation of extensive low clouds. Fig. 3 shows how EIS varies with region. In typical stratocumulus regions, e.g. along the West coast of South America, high values of EIS can be seen. But also in the higher latitudes, where mixed-phase clouds prevail, mean EIS values of 8 K and more are prominent. On the one hand, not all areas with high EIS values correlate with high positive normalised FG departures (comparing Fig. 1a with Fig. 3). For example, around 60°S where many mixed-phase clouds exist high EIS values and large negative FG departures are seen. The large negative bias is mostly likely due to a sampling issue where areas with a FG total column water vapour (TCWV) of 8 kg m^{-2} and less are screened (Geer et al., 2011). On the other hand, not all positive biases are associated with high values in EIS, as e.g. the positive FG departures in the Philippine Sea (Fig. 1a) do not have high EIS values. This is not problematic as not all areas with high positive biases are typical areas of stratocumulus clouds, but EIS seems to be a good match in subtropical stratocumulus regions.

Hence, to identify stratiform regions only regions are selected which have a large inversion strength and are dominated by liquid-phase clouds:

$$\begin{aligned} \mathrm{EIS} &> 9\,K, \\ \mathrm{IWP} + \mathrm{SWP} &< 10^{-12}\ \mathrm{kg\ m^{-2}}, \end{aligned} \tag{2}$$

with ice water path IWP and snow water path SWP. Hereby, the sum of IWP and SWP being almost zero might be overly rigorous as situations with cirrus clouds above a deck of stratocumulus are not identified

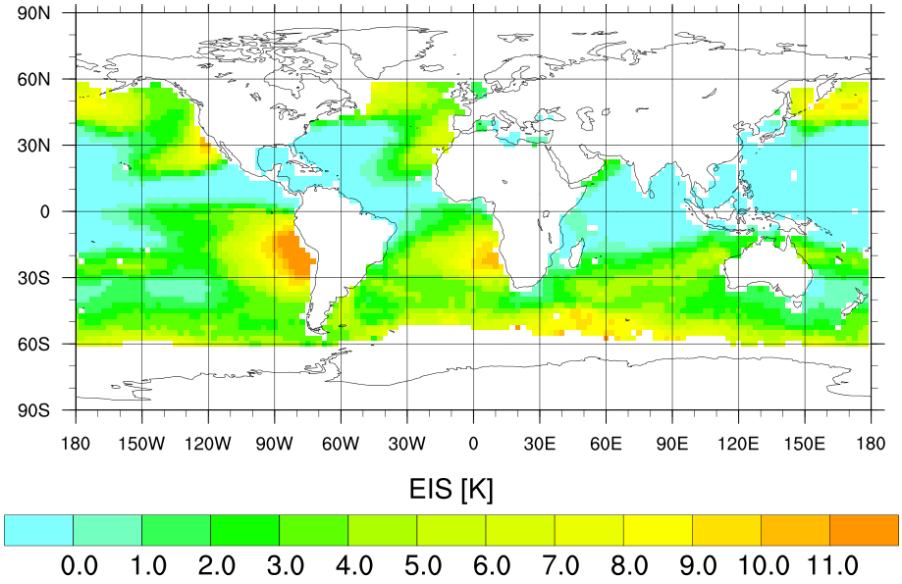

Figure 3: Map of monthly mean gridded (2.5°lat x 2.5°lon) EIS values for August 2013 using observation locations of SSMIS F-17 using IFS cycle 40R2.

by this criterion. Fig. 4 highlights areas which are identified as stratocumulus regions using criteria in Eq. (2). As it can be seen in Fig. 4a the selection criteria does not only identify typical stratocumulus regions, it does occasionally also detect areas in the mid-latitudes with high positive and negative values in normalised FG departures (Fig. 4b). Probably those are areas of stratiform low cloud amount associated with cyclonic frontal systems. One example is the region over the Indian Ocean around 40°S where there is also a long-standing positive bias, which is not understood but is relatively small compared to the bias in the stratocumulus areas. This bias is most likely due to model insufficiencies in stratiform clouds along fronts. Other reasons could be the neglected effect of atmospheric stability effects on surface emissivity (Kazumori et al., 2016) or differences between model and observed mid-latitude weather. However, most regions selected by the criteria in Eq. (2) do identify typical stratocumulus decks along the west coast of Africa, South America and California which are also marked by high positive values in normalised FG departure. When relaxing the second criterion in Eq. (2) to allow for more scenes with some e.g. cirrus characterized by little snow and/or ice amount more areas in the mid-latitudes with high positive and negative values in normalised FG departures are detected, as shown in Fig. 4c and Fig. 4d. In other words, using criteria in Eq. (2) works reasonable well to detect areas of stratocumulus.

However, using criteria in Eq. (2) does not only identify situations with a positive bias in stratocumulus areas, as shown in Fig. 5. Here, the number of occurrence of normalised FG departure is shown for the stratocumulus area off the west coast of South America [20°S - 0°, 80°W - 100°W] and how it changes when Eq. (2) has been applied. The histogram highlights that much data in this stratocumulus field with positive normalised FG departures (observations > FG) are identified. Nevertheless, some data for which the observations have lower brightness temperatures than the FG are identified by criteria in Eq. (2) as well. Actually, a map of normalised FG departures using the screening criteria as done in Fig. 1a would show minor changes compared to not using them. Even though the largest positive FG departures are removed by the screening (not shown) the shape of the histogram in Fig. 5 stays almost the same which translates into only minor changes in **mean** values of FG departures (mean normalised FG departure is 0.30 for using criteria in Eq. (2) and 0.32 for not using them calculated over the stratocumulus area off the west coast of South America). This is also highlighted by the fact that the relative number of samples

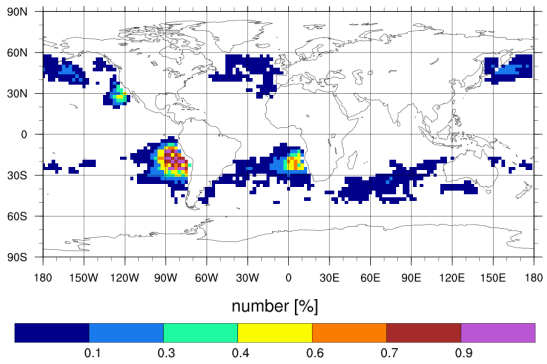

(a) Relative sample number normalised by total number of screened data using criteria in Eq. (2).

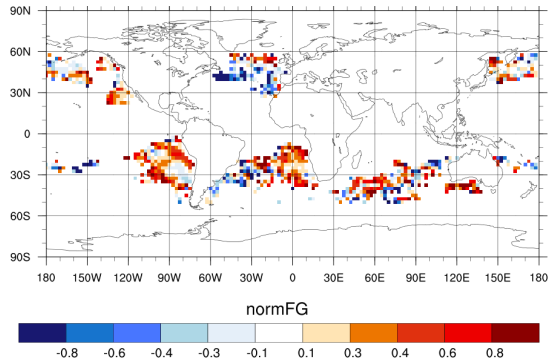

(b) Normalised FG departure in 37 GHz v-polarised for screened data using criteria in Eq. (2).

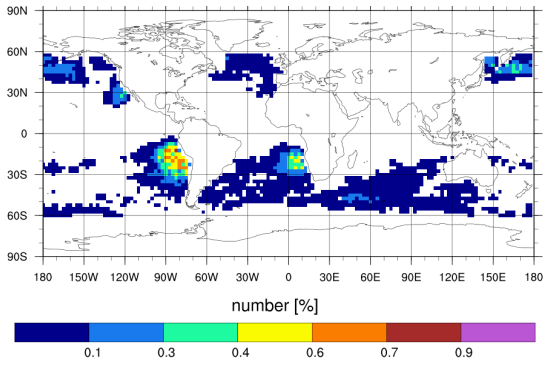

(c) Relative sample number normalised by total number of screened data with EIS >9K and IWP+SWP <0.2 kg m^{-2}.

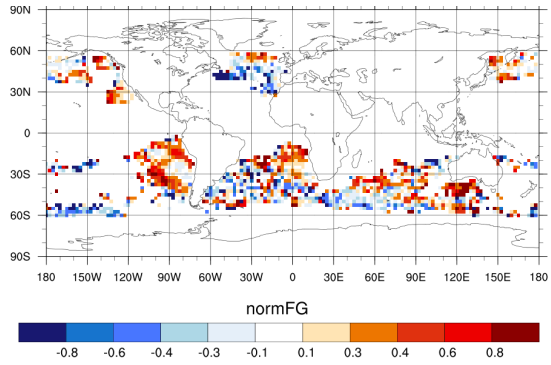

(d) Normalised FG departure in 37 GHz v-polarised for screened data with EIS >9K and IWP+SWP <0.2 kg m^{-2}.

Figure 4: Identified "stratocumulus regions" with a) & b) criteria in Eq. (2) and with c) & d) EIS >9K and IWP+SWP <0.2 kg m^{-2} using gridded data (2.5°lat x 2.5°lon) from SSMI/S F-17 for August 2013.

with positive normalised FG departures drops only by about 2% between not using criteria in Eq. (2) (69.2%) and using them (67.5%). In other words, criteria in Eq. (2) seem to identify stratocumulus areas reasonably well, however, identifying stratocumulus clouds where the model has insufficient drizzle and/or cloud liquid water compared to observations seems to be difficult.

Instead of simply screening observational data in stratocumulus areas before assimilation, a bias correction in those regions would be preferable. According to Harris and Kelly (2001) predictors are selected if they have a linear relationship with the systematic bias. Fig. 6 shows how well normalised FG departures scale with estimated inversion strength. If all samples are chosen (Fig. 6a and Fig. 6c) the mean normalised FG departure is about zero up to EIS = 8 K and then increases linearly. If only samples are chosen which contain no snow or ice clouds (Fig. 6b and Fig. 6d) the mean normalised FG departure increases linearly for EIS $>$ 0 K. This would mean EIS could potentially be a predictor for systematic biases in stratocumulus regions. It would be interesting to set up experiments in which EIS is used as a bias predictor (inside VarBC) to see if the bias in stratocumulus regions is corrected properly. However, we do not think that much could be gained by using EIS as a predictor and omitted undertaking such test because EIS is not exact at discriminating areas subject to the positive bias from those areas where the model FG is in agreement with observations, as discussed before (see Fig. 5). Even though high values in EIS can be associated with subtropical stratocumulus clouds, the model bias in stratiform clouds cannot

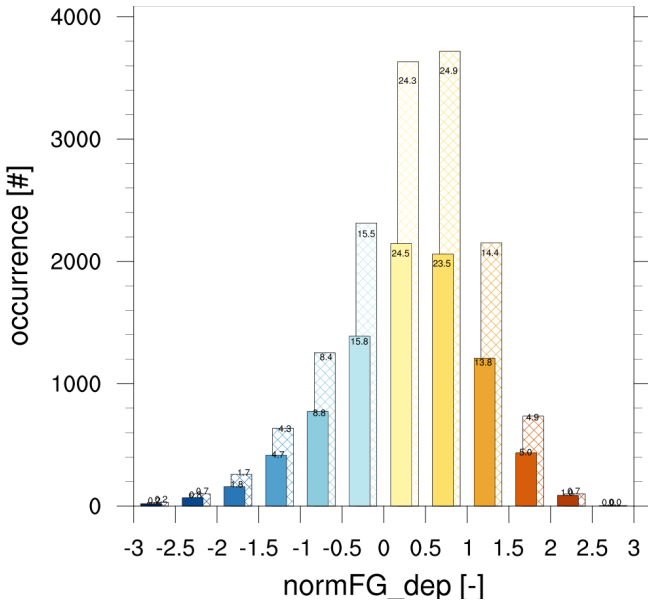

Figure 5: Histogram of normalised FG departure within the typical stratocumulus region off the West coast of South America [20°S - 0°, 80°W - 100°W] using criteria in Eq. (2) (solid bars) and not using them (hatched bars). Binning is done for every 0.5 normalised FG departure. The number at the top of the bar represents the number of data of this bin relative to the total number of all bins in %. Data comes from SSMI/S F-17 at 37 GHz, v-polarised during August 2013.

be associated with high EIS values in all cases. The model seems to capture some parts of stratocumulus clouds very well while other parts are not as cloudy as observed. This makes it quite difficult to use EIS as proper predictor, which can also be seen in the large spread in normalised FG departures (Fig. 6a and Fig. 6b) or in small negative FG departures with high EIS values around 25°S, 80°W (Fig. 4b). In current operations EIS is used to detect stratocumulus regions, where then consequently shallow convection is switched off. Despite a strong inversion in the PBL (measured by EIS, as explained in this section) other factors seem to influence properties of stratocumulus as well, which probably explains why using EIS in Eq. (2) captures a variety of situations where observations and model agree and disagree. This unstable behaviour of EIS and the open question if EIS is robust and well predicted by the model itself challenges its use as a bias predictor even more.

3 Screening of stratocumulus regions

Nevertheless, because criteria in Eq. (2) are reasonable in detecting stratocumulus areas, where the model has often problems in generating enough clouds and/or drizzle, it can be tested if the screening of MWI observations in those areas affects the forecast scores. For this purpose two 40R2 experiments with a resolution of TL511 have been set up covering the time period of six months between 1 July and 31 December 2013 which delivers robust statistical results. The first experiment is a control run **(control)** using the full operational set of observations including the two all-sky imagers SSMIS F-17 and TMI, which have been actively assimilated at this time. The setup of the second experiment is equal to **control** but excluding MWI data of SSMIS F-17 and TMI in stratocumulus regions according to Eq. (2) **(Sc off)**. This section investigates the effects of screening MWI observations in stratocumulus decks on mean

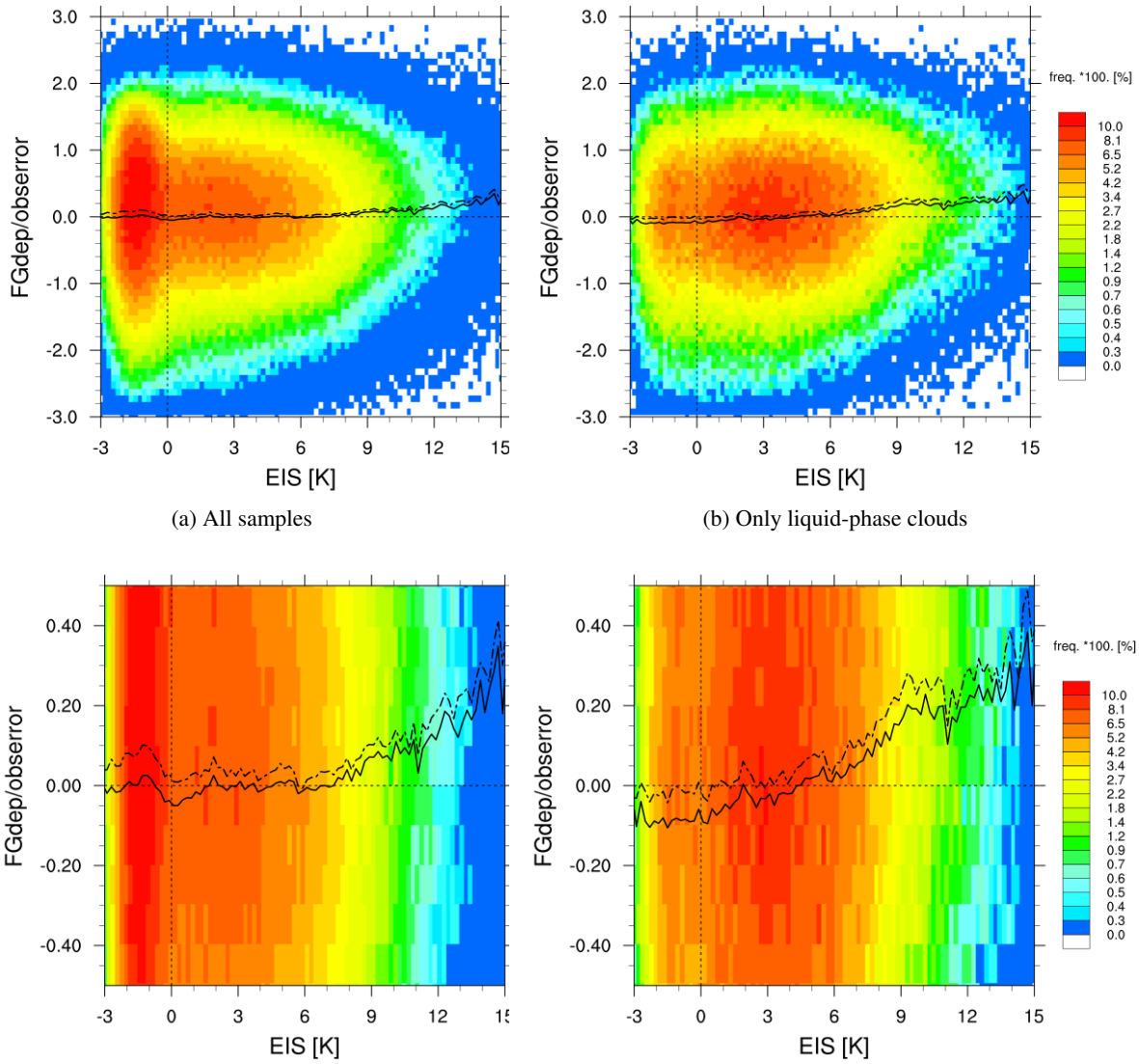

(a) All samples

(b) Only liquid-phase clouds

(c) Zoom into 6a

(d) Zoom into 6b

Figure 6: Contour plot of relative number of occurrence as a function of EIS and normalised FG departure. The mean (solid line) and median (dashed line) normalised FG departures are calculated for every 0.2 K bin in EIS. Data comes from SSMIS F-17 at 37 GHz, v-polarised during August 2013.

changes in humidity and temperature and on global forecast scores and the verification with observations.

3.1 Mean change in analysis and forecast at 850 hPa

By screening microwave imager observations in stratocumulus areas we can see that the relative humidity in the analysis (forecast day = 0) is reduced at 850 hPa (roughly the height of stratocumulus clouds) in the tropics with the temperature slightly increased and the specific humidity slightly decreased for **Sc off**, as shown in Fig. 7. For T+12 h to T+48 h humidity and temperature do show mean changes compared to **control**. However, for T+72 h onwards (ranging into the medium-range forecast) differences between

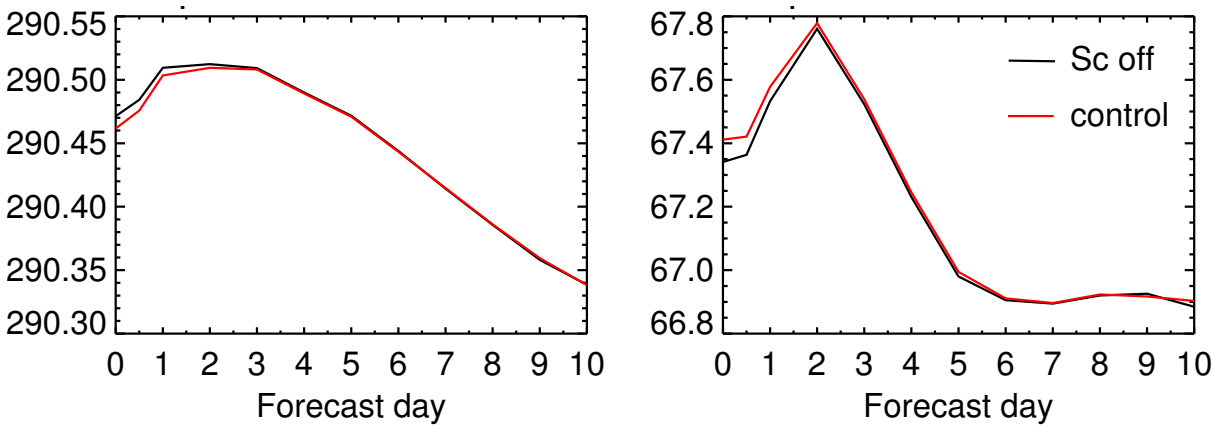

(a) Temperature

(b) Relative humidity

Figure 7: Change in field mean in a) temperature [K] and b) in relative humidity [%] at 850 hPa for tropics (20°S to 20°N). Data comes from **control** and **Sc off** between July to December 2013.

the mean fields in humidity and temperature are almost negligible. That those mean changes in humidity and temperature for short-range forecasts are very localised to the stratocumulus regions for which MWI observations have been screened in **Sc off** can be seen in Fig. 8 and Fig. 9, respectively. Here, there is no spread in those mean changes for T+12 to T+48 to other areas or height levels (not shown), i.e. the mean drying at around 850 hPa occurs only for stratocumulus regions where MWI data has been screened in **Sc off** up to forecast day 2.

3.2 Global forecast scores

To study how global forecast scores are affected we look at the change in the root-mean-square of forecast error (RMSE) of different variables. A decrease in RMSE would usually be interpreted as an improvement and an increase in RMSE as a degradation in forecast scores for **Sc off**. However, as shown later one has to be careful with this interpretation. Fig. 10 shows the normalised difference in RMSE at 850 hPa in humidity between **Sc off** and **control**. Here, the T+12 h own analysis RMSE actually represents the RMS of the analysis increment. That means if the analysis increments become smaller, the RMSE will also appear smaller. A decrease in the analysis increment is seen in the typical stratocumulus areas for **Sc off**, which might be not surprising. For **Sc off** less imager data which is sensitive e.g. to humidity is assimilated in those areas. Fewer microwave imager observations would then reduce the difference between analysis and FG for **Sc off**.

Throughout the forecast time the RMSE in humidity stays decreased in those stratocumulus areas (East coast of Africa, California and South America), which is also true for temperature (Fig. 11). A decrease in RMSE for wind is seen for T+12 h to T+24 h (not shown). A similar behaviour can also be seen for surface fields but not for higher levels (e.g. Fig. 11). It is interesting that the RMSE only reduces locally without propagating into space or to higher levels during the forecast, which raises questions whether a screening of stratocumulus areas is necessary in the first place. Furthermore, the corresponding maps of changes in standard deviation (not shown) look very much like changes in RMSE, which indicates that the variability of the analysis and of the forecast in stratocumulus areas is decreased for **Sc off** and not the mean analysis or mean forecast. As shown in section 3.1, this is true for forecast times T+72 h and

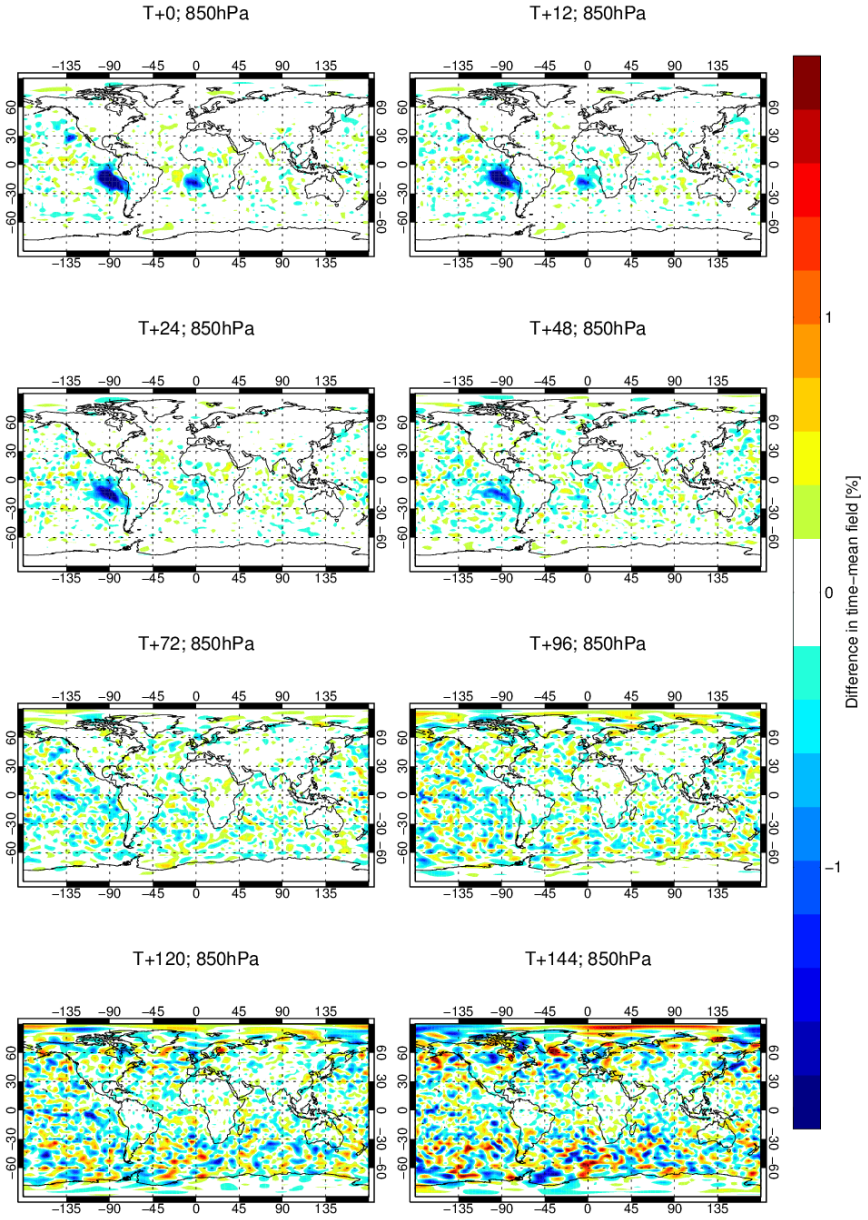

Figure 8: Maps of mean change (= difference in time-mean field between **Sc off** and **control**) in humidity at 850 hPa for different forecast times. Blue colours represent a decrease in humidity and red colours an increase in humidity for **Sc off**. Results cover the time period from 1st July 00 UTC to 31st December 2013 12 UTC.

longer.

A reason for this very local reduction of RMSE in stratocumulus areas could be due to a change in the analysis instead of the forecast, which would prevent a spread in time and space. To test this hypothesis we have looked at forecast scores verified with the operational analysis instead of own analysis. If no reduction in RMSE in stratocumulus regions are seen with forecast time when using the operational analysis then the change in own-analysis RMSE is measuring a change in the mean or variability of the

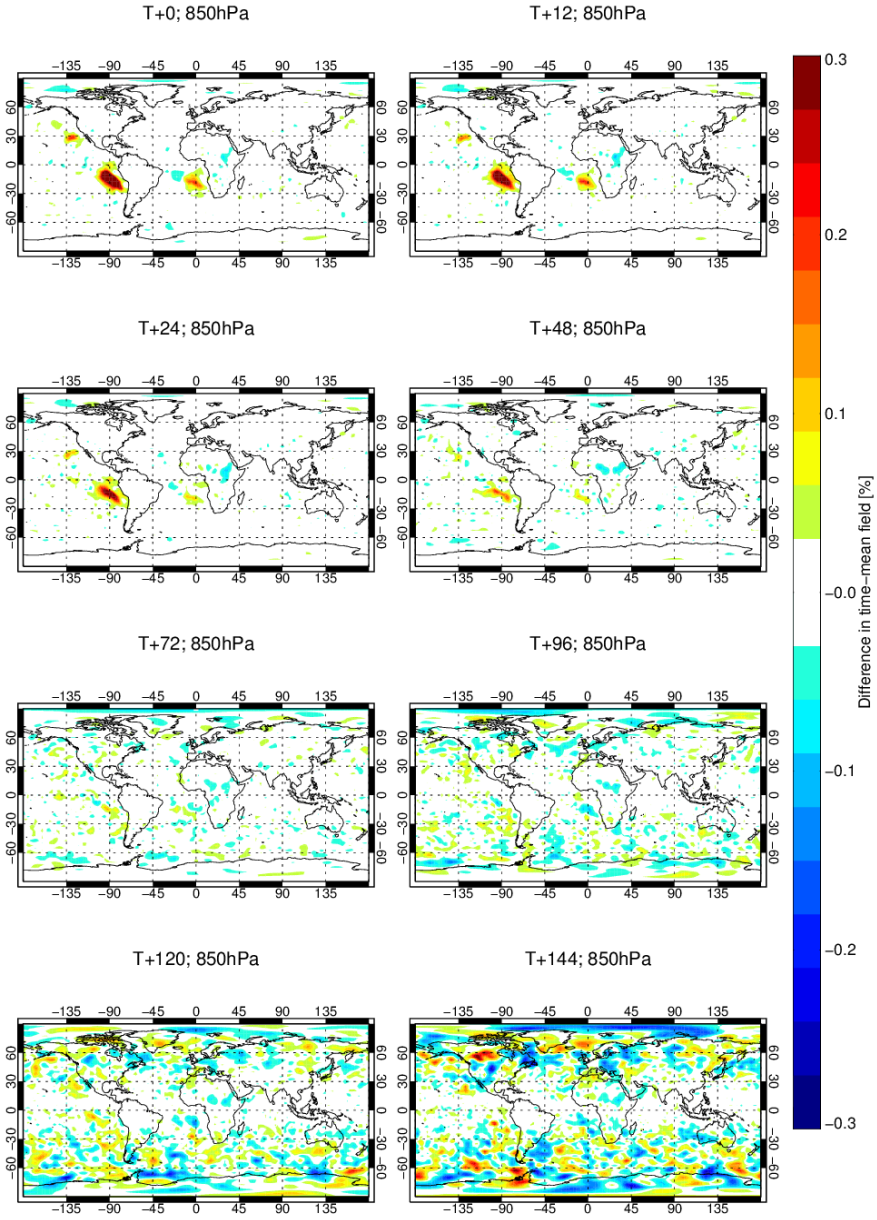

Figure 9: Maps of mean change (= difference in time-mean field between **Sc off** and **control**) in temperature at 850 hPa for different forecast times. Blue colours represent a decrease in temperature and red colours an increase in temperature for **Sc off**. Results cover the time period from 1st July 00 UTC to 31st December 2013 12 UTC.

analysis rather than of the forecast. Indeed, no obvious reduction in RMSE for humidity or temperature for various height levels is seen for **Sc off** (not shown). Only for T+12 the RMSE (= increment of FG and operational analysis) is locally reduced in stratocumulus regions. That means, mostly the variability of the analysis is decreased with only very localised mean changes in humidity and temperature for the short-range forecast up to T+48 h (Fig. 8 and Fig. 9, respectively), which do not spread.

Looking at mean changes in RMSE in the northern hemisphere, tropics and southern hemisphere high-

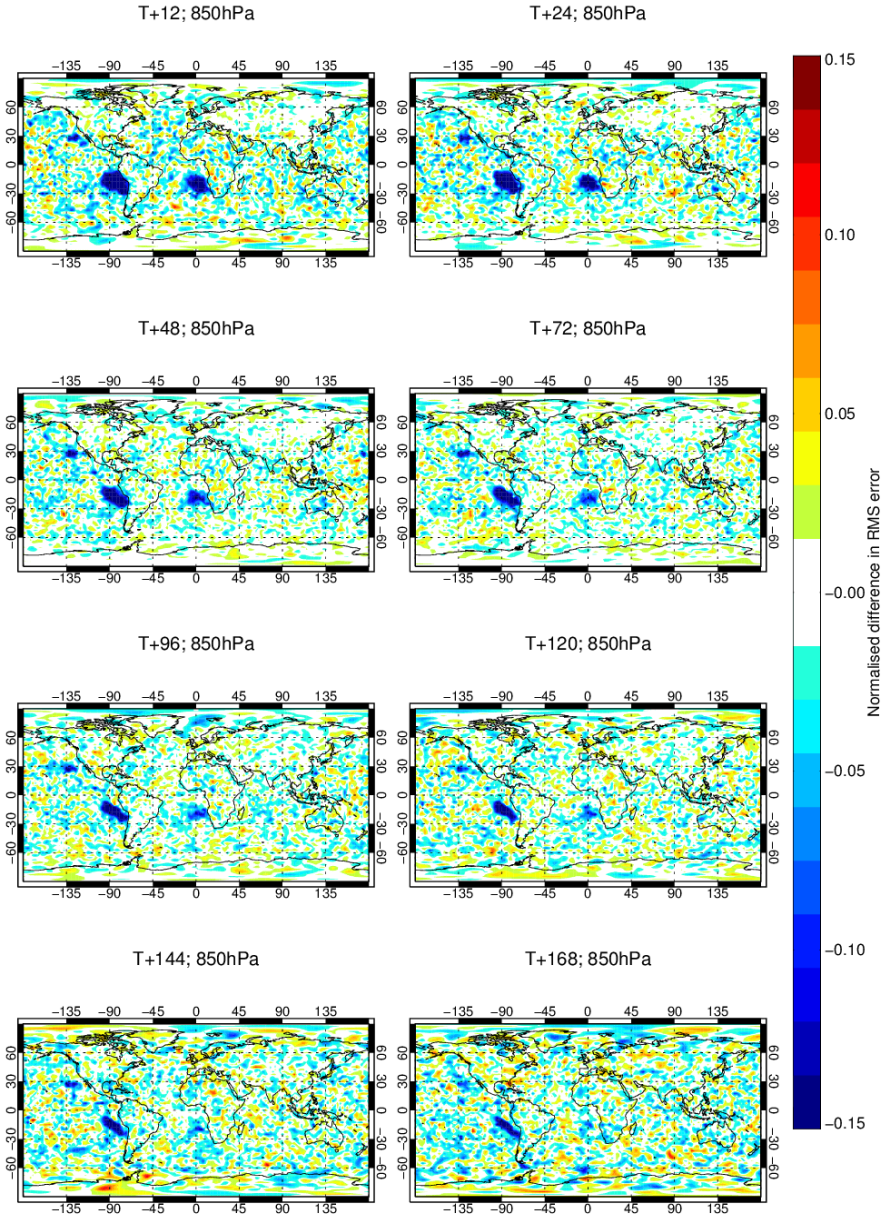

Figure 10: Maps of the differences in RMSE in humidity at 850 hPa between **Sc off** and **control** normalised by **control** for different forecast times. Blue colours represent a decrease in RMSE and red colours an increase in RMSE for **Sc off**. Results cover the time period from 1st July 00 UTC to 31st December 2013 12 UTC.

lights how the variability of the analysis changes for medium-range forecasts when MWI observations are screened in stratocumulus areas. An example is displayed in Fig. 12a, which shows the normalised difference in RMSE of relative humidity at 850 hPa between **Sc off** and **control** using own-analysis verification. It is noticeable that for all regions the RMSE decreases significantly for **Sc off**. For the northern and southern hemisphere RMSE decreases up to day 3 and 4, respectively. For the tropics the RMSE is decreased throughout the forecast time. Similar features can be found for RMSE of humidity at 1000 hPa

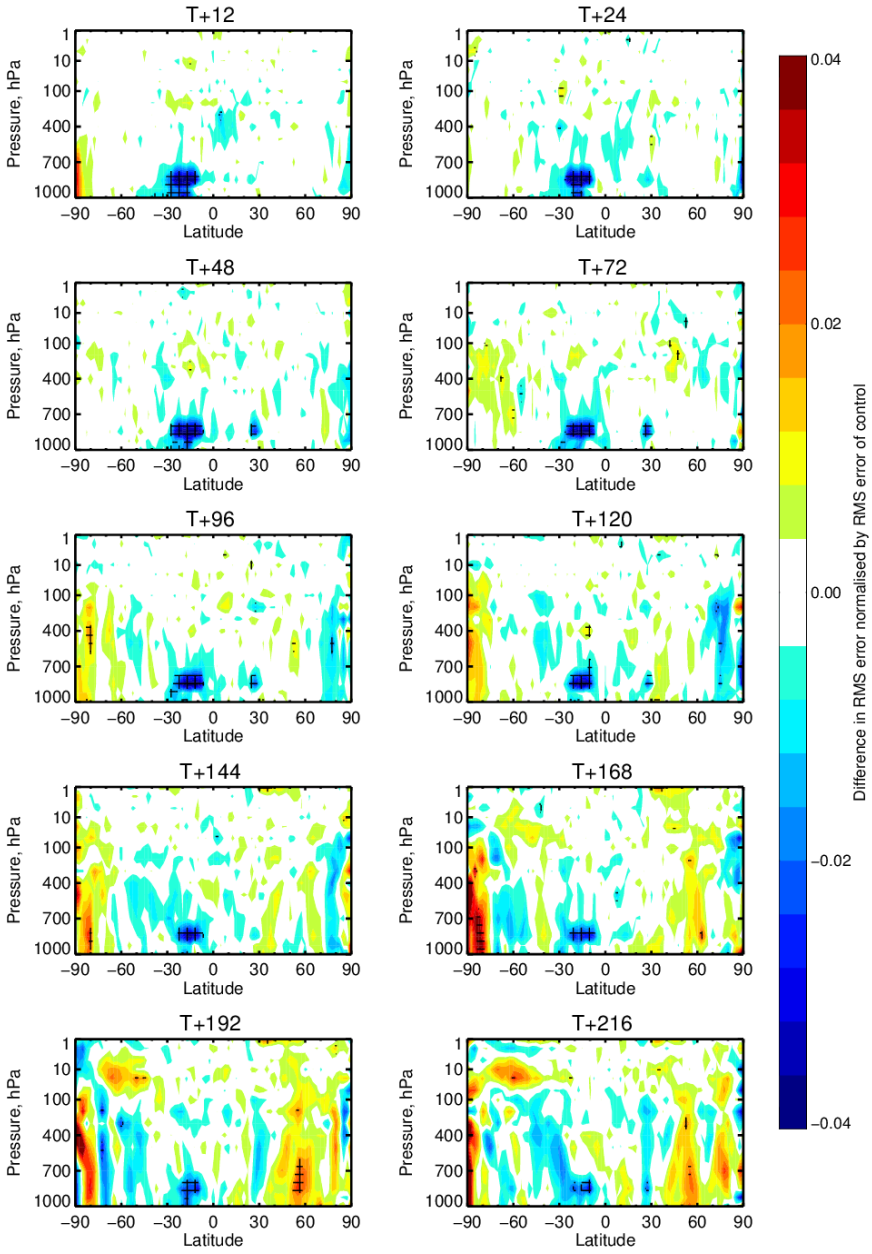

Figure 11: Zonal averages of differences in RMSE in temperature between **Sc off** and **control** normalised by **control** at different height levels for different forecast times. Blue colours represent a decrease in RMSE and red colours and increase in RMSE for **Sc off**. Results cover the time period from 1st July 00 UTC to 31st December 2013 12 UTC.

(not shown), however, the magnitude is not as large. Interestingly, changes in RMSE do almost look like changes in standard deviation of forecast errors (Fig. 12b). Additionally, the mean error only changes slightly for height levels up to 500 hPa (not shown). Using the operational analysis as a reference (compared to using the own analysis) does not show a significant change in RMSE for day 2 and longer, as displayed in Fig. 12c. Only for T+12 h a decrease in the tropics and for T+12 h to T+24 h an increase in the RMSE in the northern and southern hemisphere can be seen. Overall, only small positive and neg-

ative differences in own-analysis RMSE exist which can be related to small changes in the mean fields in the short-range and changes in the variability of the analysis for longer forecast times. These changes cannot be interpreted as good or bad, but there is clearly a loss of information going into the analysis when MWI observations are screened in stratocumulus areas.

3.3 Observational verification

To verify the data screening in stratocumulus regions for the short-range forecast, fits to observations are checked. Fig. 13 shows the change in standard deviation of FG departure between **Sc off** and **control** for various instruments in the tropics (20°S to 20°N). Many temperature sensitive observations, e.g. from the Infrared Atmospheric Sounding Interferometer (IASI, not shown) and the Advanced microwave sounding unit-A (AMSU-A, from Aqua, NOAA-15, NOAA-16, NOAA-18, NOAA-19, Metop-A and Metop-B, Fig. 13c) show a neutral behaviour when MWI data in stratocumulus areas is screened. For humidity sensitive observations the observational fits are slightly degraded for **Sc off**. For example, degradations can be seen in high tropospheric water vapour channels 11-12 of the High-resolution Infrared Radiation Sounder (HIRS, from NOAA-19 and Metop-A, not shown), channels 18-20 of the Advanced Technology Microwave Sounder (ATMS, from NPP, Fig. 13a) and low peaking water vapour channels 4-5 from the Microwave Humidity Sounder (MHS, from NOAA-18, NOAA-19, Metop-A and Metop-B, Fig. 13b). That means, it is actually beneficial to assimilate MWI data from stratocumulus areas despite the model bias.

The change in standard deviation in FG departure for humidity sensitive observations is interesting on its own because it could suggest that biases in stratocumulus areas are also related to biases in the water vapour. Looking into maps of FG departures for 22 GHz which is very sensitive to humidity actually confirms this suspicion. In regions of typical stratocumulus clouds positive biases in 22 GHz can be found (not shown), which are partly seen in 37 GHz from SSMIS-F17 (see Fig. 1a) as well. However, this in only true for IFS cycle 40R2 and not for the newer IFS cycles 41R2 or 43R1 where a bias in stratocumulus areas still exists. Here, corresponding maps of FG departures in 22 GHz do not show any bias, which suggest that the additional use of all-sky sensors sensitive to humidity and cloud might have constrained the humidity field better than in the past. In other words the positive FG departure must mainly be related to difference in liquid water (cloud or drizzle) in stratocumulus areas.

The only improvement in observational fits when MWI data in stratocumulus areas is screened can be seen for atmospheric motion vectors (AMVs) in lower levels in the tropics (Fig. 13d). However, it could be questioned if this is a genuine improvement because other wind observations do not show the same signal (not shown). For example, Lonitz and Horvath (2011) showed that the height assignment of AMVs in stratocumulus areas can be too low which is related to the presence of the planetary boundary layer inversion. In other words, the detected wind can be assigned to erroneously low heights. In case of no complementary observations in stratocumulus areas the model would try to fit those "wrong" low-level winds. However, if other observational constraints exist in stratocumulus areas, e.g, MWI data, the fit to AMVs could be weaker. An alternative hypothesis would be that possibly erroneous wind adjustments may be created to fit observed cloud and humidity fields, but even if this is true, the effect is not intensifying and spreading into other areas and heights, as it can be seen e.g. in maps of mean changes of wind at various height levels for T+12 h (not shown). The real causes for the improvement in the low-level AMVs needs to be better understood to clarify if the outlined hypothesis hold true or not.

Changes in observational fits of MHS, AMSU-A and AMVs in the stratocumulus area off the west coast of South America [20°S - equator, 80°W - 100°W] are displayed in Fig. 14. Here, no significant changes in the standard deviation of FG departure are seen for most cases. Only, for channel 5 of MHS and

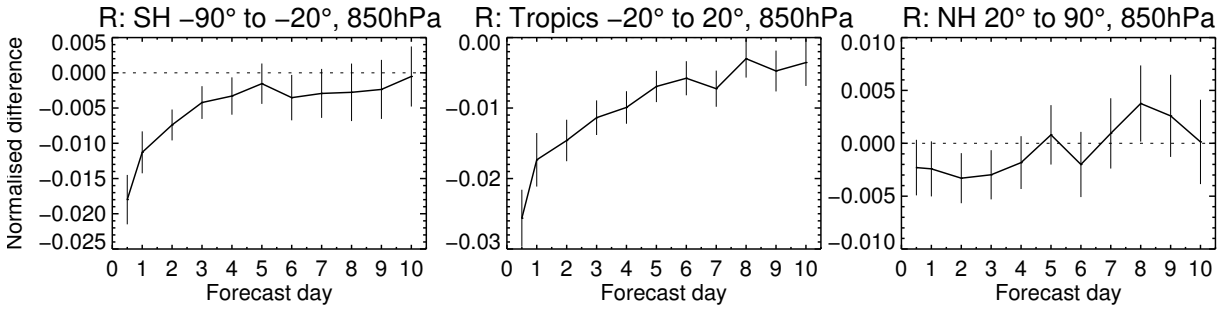

(a) RMSE with reference = own analysis.

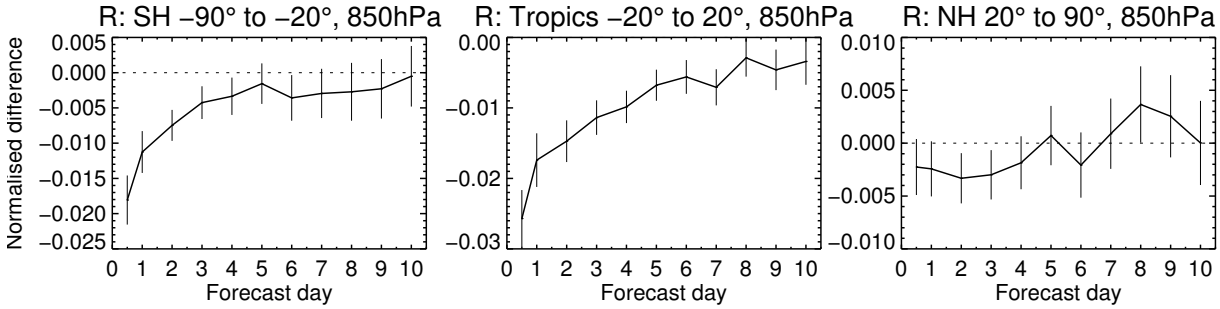

(b) Standard deviation with reference = own analysis.

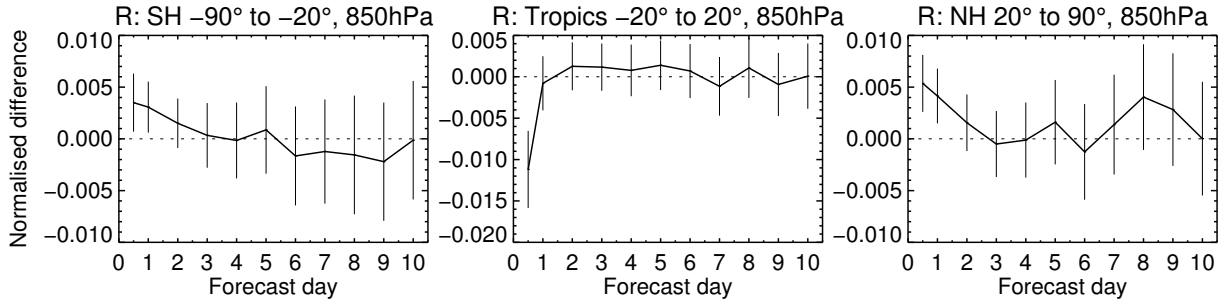

(c) RMSE with reference = operational analysis.

Figure 12: Difference in RMSE (a) with reference = own analysis, c) with reference = operational analysis) and b) standard deviation (with reference = own analysis) between **Sc off** and **control** for relative humidity at 850 hPa normalised by **control** for different regions. Negative values indicate smaller values for **Sc off**. Results cover the time period from 1st July 00 UTC to 31st December 2013 12 UTC.

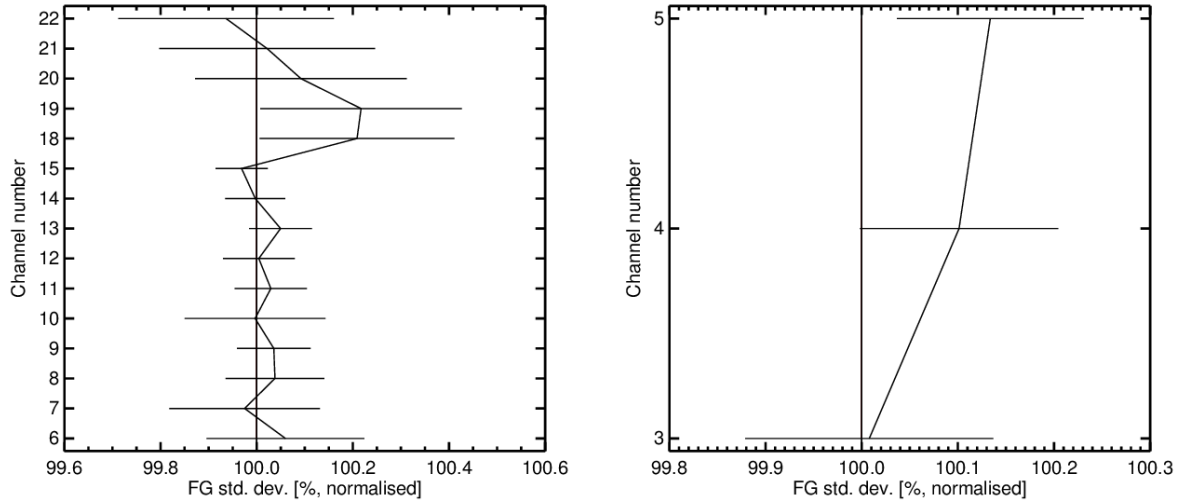

(a) ATMS (from NPP)

(b) MHS (from NOAA-18, NOAA-19, Metop-A and Metop-B)

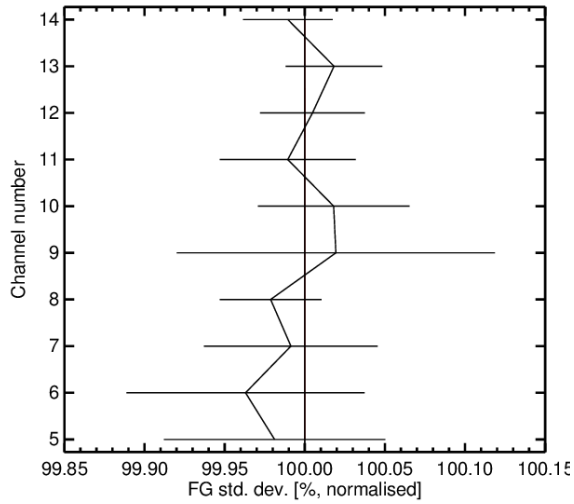

(c) AMSU-A (from Aqua, NOAA-15, NOAA-16, NOAA-18, NOAA-19, Metop-A and Metop-B)

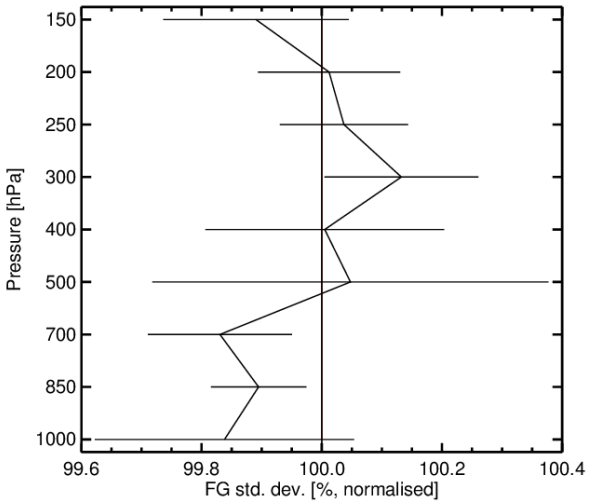

(d) Atmospheric motion vectors

Figure 13: Normalised difference in standard deviation of first-guess departures between **Sc off** and **control** for different instruments in the tropics. The normalisation is done with results from **control**. Values less than 100% would indicate beneficial impacts from screening MWI data in stratocumulus areas. The horizontal bars indicate 95% confidence range. Results cover the time period from 1st July 00 UTC to 31st December 2013 12 UTC.

channel 5 and 14 of AMSU-A a significant degradation can be seen when no MWI data in stratocumulus areas is used. Channel 5 of MHS is the lowest peaking humidity soundings and, hence, would be expected to be most sensitive to changes induced by the screening of stratocumulus clouds. Channel 5 of AMSU-A is a low peaking temperature sounding channel and channel 14 of AMSU-A is the highest peaking temperature sounding channel. The reason why such a change in standard deviation of FG departure happens here has to be investigated further. Small reductions in channel 8 of AMSU-A and at 700 hPa for AMVs are also seen. Here, it could be argued again that the slight reduction for AMVs is not genuine as stated above. Nevertheless, in summary we can say that the assimilation of MWI data in stratocumulus areas is unproblematic or can even be beneficial for the short-range forecast.

4 Summary

In areas of stratocumulus clouds it is believed that the IFS model does not have enough drizzle or cloud water compared to observations, despite recent modifications in IFS cycle 43R1 intended to address these biases. This results in a systematic positive bias of a few Kelvin in the microwave brightness temperatures (especially seen at the West coast of Africa in Fig. 2). Usually systematic biases are addressed through bias correction. If no proper bias correction exists the data is usually screened before assimilation, e.g. microwave imagery in cold-air outbreaks (Lonitz and Geer, 2015) to prevent the bias being assimilated, and potentially damaging forecasts. Despite the systematic model bias in stratocumulus areas observations from MWI have been assimilated with no specific stratiform bias correction predictor in place.

In this study, areas of stratocumulus have been identified using the estimated inversion strength (EIS), which has been shown to be a useful measure for periods of moderate tropospheric subsidence (Wood and Bretherton, 2006). The formation of extensive low-level cloud decks, e.g. stratocumulus is related to subsidence. For EIS > 9 K and only liquid-phase clouds, areas of typical stratocumulus along the West coast of Africa and North and South America could be identified, although rarely some mid-latitudes areas which are not known to be typical stratocumulus areas were identified. Those incidents with high EIS and positive FG departures are most likely linked to stratiform low cloud amount in frontal systems. In other words, the criteria in Eq. (2) work reasonably well to detect stratiform clouds, however, in the future other criteria based also on lower-troposphere stability could even be better in discriminating biased stratocumulus areas. One example would be a combination of LTS and vertical velocity as done by Medeiros and Stevens (2011). They used these criteria to select stratocumulus fields in their Aquaplanet simulation.

It was also shown that the normalised FG departure scales linearly with EIS in areas with only liquid-phase clouds. This relationship could be exploited to see if the inversion strength could be used as a predictor in variational bias correction in the future. Nevertheless, we do not think that much could be gained by using EIS as a predictor because the model seems to capture some parts of stratocumulus clouds very well while other parts are not as cloudy as observed. EIS is not able to discriminate well enough the areas of bias from those areas unaffected.

Another option to prevent potential degradations of forecast scores could have been a screening of MWI data in stratocumulus areas which show a bias. In this study, a reduction in own analysis RMSE in humidity and temperature could be found when stratocumulus areas have been screened, however, this reduction does not propagate to other areas or height levels with forecast time and has been identified to be a change in the analysis and short-range forecast in very localised stratocumulus areas. That means, medium-range global forecast scores are unaffected by a stratocumulus screening. Fits to observations

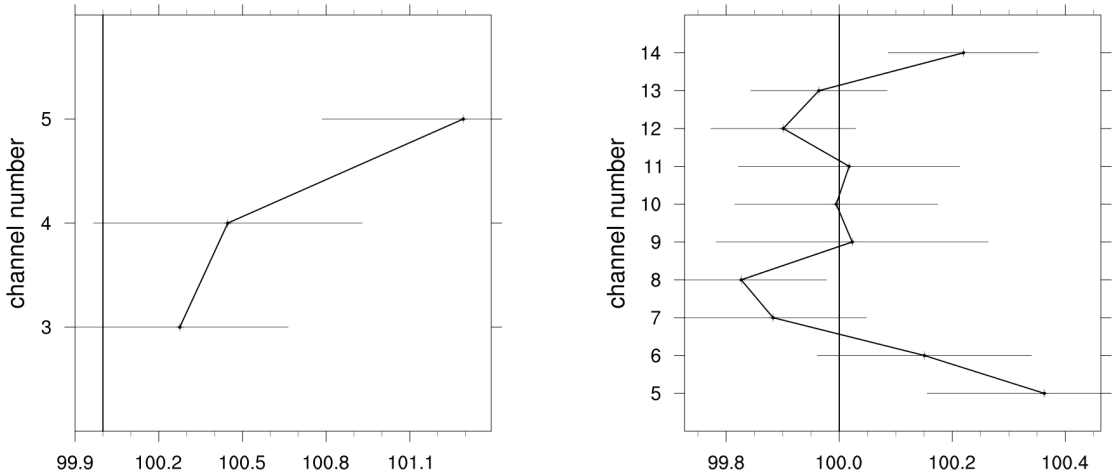

(a) MHS (from NOAA-18, NOAA-19, Metop-A and Metop-B)(b) AMSU-A (from Aqua, NOAA-15, NOAA-16, NOAA-18, NOAA-19, Metop-A and Metop-B)

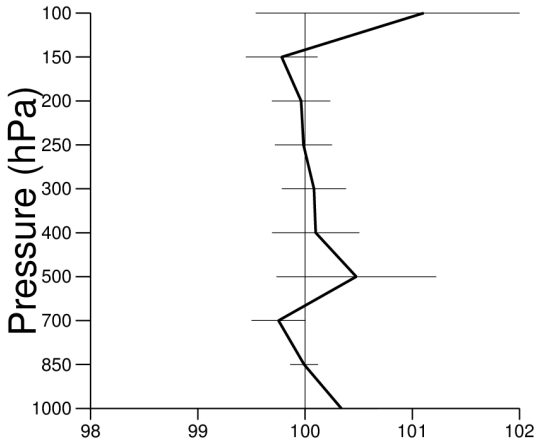

(c) Atmospheric motion vectors

Figure 14: Normalised difference in standard deviation of first-guess departures between **Sc off** and **control** for different instruments between 20°S - equator and 80°W - 100°W. The normalisation is done with results from **control**. Values less than 100% would indicate beneficial impacts from screening MWI data in stratocumulus areas. The horizontal bars indicate 95% confidence range. Results cover the time period from 1st July 00 UTC to 31st December 2013 12 UTC.

show that the stratiform screening has a neutral effect on temperature, but degradations in humidity and an improvement in wind, which might not be genuine. In conclusion, observations in stratocumulus areas are probably useful for the assimilation system and probably do not cause any degradations. Despite a systematic bias between model and observations they should, therefore, not be screened. The continuation of actively assimilating this data will also keep the focus on improving the quality of stratocumulus in the forecast model.

Acknowledgements

Peter Bechthold is thanked for fine tuning a subroutine which calculates the estimated inversion strength. Katrin Lonitz's work at ECMWF is funded by the EUMETSAT fellowship programme.

References

M. Kazumori, A. J. Geer, and S. J. English. Effects of all-sky assimilation of GCOM-W/AMSR2 radiances in the ECMWF numerical weather prediction system. *Q.J.R. Meteorol. Soc.*, 142(695):721–737, 2016.

R. Buizza, J-R Bidlot, M. Janousek, S. Keeley K., Mogensen, and D. Richardson. New IFS cycle brings sea-ce coupling and higher ocean resolution. *ECMWF Newsletter*, (150):14–17, 2017.

K. Lonitz and A. Geer. EUMETSAT/ECMWF Fellowship Programme Research Report: New screening of cold-air outbreak regions used in 4D-Var all-sky assimilation. Technical report, ECMWF, 2015.

R. Wood and C. S. Bretherton. On the relationship between low cloud cover and lower-tropospheric stability. *Journal of Climate*, 19:6425–6432, 2006.

J. M. Slingo. The development and verification of a cloud predictor scheme for the ECMWF model. *Quart. J. Roy. Meteor. Soc.*, 113:899–927, 1987.

S. A. Klein and D. L. Hartmann. The seasonal cycle of low stratiform clouds. *Journal of Climate*, 6: 1588–1606, 1993.

R. Wood and D. L. Hartmann. Spatial variability of liquid water path in marine boundary layer clouds: The importance of mesoscale cellular convection. *Journal of Climate*, 19:1748–1764, 2006.

A. J. Geer, R. Forbes, P. Bauer, and F. Baordo. Big temperature increments in the 37r3 esuite coming from all-sky observations in the southern winter. Technical Report File: R43.8/AG/11110, ECMWF, 2011.

B. A. Harris and G. Kelly. A satellite radiance-bias correction scheme for data assimilation. *Q.J.R. Meteorol. Soc.*, 127(574):1453–1468, 2001.

K. Lonitz and A. Horvath. Comparison of MISR and Meteosat-9 cloud-motion vectors. *Journal of Geophysical Research*, 116:D24202, 2011.

B. Medeiros and B. Stevens. Revealing differences in GCM representations of low clouds. *Climate Dynamics*, 36(1):385–399, 2011.